EUROPEAN FUSION DEVELOPMENT AGREEMENT

EFDA–JET–PR(04)24

T. Onjun, A. H. Kritz, G. Bateman, V. Parail, H. R. Wilson, A. Dnestrovskij
and JET EFDA contributors

Interplay between Ballooning and Peeling Modes in Simulations of the Time Evolution of ELMs

Interplay between Ballooning and Peeling Modes in Simulations of the Time Evolution of ELMs

T. Onjun[1], G. Bateman[1], A. Dnestrovskij[2], A. H. Kritz[1], V. Parail[3], H. R. Wilson[3], and JET EFDA contributors*

[1]LehighUniversity Physics Department, 16 Memorial Drive East, Bethlehem, PA 18015
[2]Russian Science Centre Kurchatov Institute, Moscow, Russian Federation
[3]EURATOM/UKAEA Fusion Association, Culham Science Centre, Abingdon Oxon OX14 3DB, UK
** See annex of J. Pamela et al, "Overview of Recent JET Results and Future Perspectives", Fusion Energy 2002 (Proc. 19th IAEA Fusion Energy Conference, Lyon (2002).*

Preprint of Paper to be submitted for publication in
Physics of Plasmas

ABSTRACT

The time evolution of Edge Localized Modes (ELMs) in the JET tokamak [P. H. Rebut *et al.*, Nucl. Fusion **25**, 1011 (1985)] is investigated using the JETTO predictive modeling code [M. Erba *et al.*, Plasma Phys. Control. Fusion **39**, 261 (1997)]. It is found that both pressure-driven ballooning and current-driven peeling modes can play a role in triggering the ELM crashes. In the simulations carried out, each large ELM consists of a sequence of quasi-continuous small ELM crashes. Each sequence of ELM crashes is separated from the next sequence by a relatively longer ELM-free period. The initial crash in each ELM sequence can be triggered either by a pressure-driven ballooning mode or by a current-driven peeling mode, while the subsequent crashes within that sequence are triggered by current-driven peeling modes, which are made more unstable by the reduction in the pressure gradient resulting from the initial crash. The HELENA and MISHKA ideal MHD stability codes [A. B. Mikhailovskii *et al.*, Plasma Phys. Rep **23**, 713 (1997)] are used to validate the stability criteria used in the JETTO simulations. This stability analysis includes infinite-n ideal ballooning, finite-n ballooning, and low-n kink/peeling modes. The simulations and the associated stability analysis may lead to an improved understanding of the physical mechanisms that control the evolution of ELMs.

1. INTRODUCTION

The improved confinement regime in tokamaks known as the high confinement mode (H-mode) is often perturbed by the onset of quasi-periodic bursts of MHD activity and D_α emission at the edge of the plasma known as edge localized modes (ELMs). Each ELM crash results in a rapid loss of particles and energy from the edge of the plasma, which reduces the average global energy content by up to 10 % [1]. Furthermore, these transient bursts of energy and particles into the scrape-off layer produce high peak heat loads on the divertor plates. On the other hand, the ELMs play an important role in removing excessive heat and particles, as well as impurities from the region near the separatrix. It is generally accepted that ELMs control the plasma parameters at the top of the pedestal in H-mode plasmas. The pedestal, in turn, has a strong influence on the energy confinement of tokamak plasmas due to observed stiffness in the ion and electron temperatures [2]. Consequently, ELMs are likely to affect the performance in burning plasma experiments such as the International Thermonuclear Experimental Reactor (ITER) [3], and it is important to understand the physical mechanisms that trigger ELM crashes.

As the plasma makes the transition from the low confinement mode (L-mode) to the H-mode, a steep pressure gradient, called the pedestal, develops in a region at the edge of the plasma. This steep pressure gradient results in an increase in the bootstrap current within the pedestal. The increase in the edge pressure gradient and in the edge current density leads to a destabilization of MHD modes, which results in a loss of plasma energy and particles to the wall. The destabilization is believed to be caused either by a pressure-driven ballooning mode [4, 5] or by a current-driven peeling mode [1, 6, 7, 8, 9]. The pressure-driven ballooning mode becomes unstable when the pressure gradient exceeds a critical pressure gradient, while the current-driven peeling mode occurs when the current density exceeds a critical current density. The effects of ELMs in simulations of H-mode plasmas have been considered in a number of papers [10, 11, 12, 13, 14]. In core-edge simulations carried out using the JETTO code [10, 11, 12] and the ASTRA code [13], only the pressure-driven ballooning mode was considered as an ELM trigger. However, it was found in Ref. [14] that a current-driven peeling mode can also play a role in triggering the ELM crashes that limit the pressure at the top of the pedestal. JETTO simulations indicate that the interaction of physical processes involving ELMs triggered by a current-driven peeling mode cause the pressure at the top of the pedestal to increase with heating power as observed in experiment [14].

In this paper, the JETTO code is used to carry out simulations of the core and edge plasmas with parameters similar to those appropriate for JET discharges. In these simulations, an ELM crash is triggered either by a pressure-driven ballooning mode or by a current-driven peeling mode, depending on which mode reaches its stability limit first. The MHD equilibrium and stability analyses codes, HELENA and MISHKA [15], are used to evaluate the edge stability of the plasma just before an ELM crash in order to confirm the validity of the simplified stability criteria used to trigger ELMs in the JETTO simulations. The instabilities included are the infinite-n ideal ballooning, the finite-n ballooning, and the low-n kink/peeling modes. JETTO simulates the time evolution of

the main plasma parameters both during and between ELMs. The goal in carrying out the JETTO simulations and the associated MHD stability investigation is to obtain a better understanding of the evolution of ELMs.

This paper is organized as follows. The codes used in the study, JETTO, HELENA and MISHKA, are briefly described in Section 2. The criteria for triggering ELM crashes in the JETTO simulation are given in Section 3. Simulation results and a stability analyses are presented in Section 4, followed by conclusions in Section 5.

2. CODES USED IN THE STUDY

In this paper, simulations are carried out using predictive JETTO code, while the MHD stability analyses involve use of the HELENA and MISHKA codes. These codes are described in this section.

2.1. THE JETTO CODE

The JETTO $1\frac{1}{2}$D transport code [16] is used to evolve the plasma current, temperature and density profiles in both the core and pedestal regions. The core transport is calculated using the Mixed Bohm/gyro-Bohm model [17]. The pedestal in the JETTO simulation is produced by assuming that the turbulent transport is suppressed in the region between the top of the pedestal and the separatrix. For simplicity, all the diagonal elements of the transport matrix within the pedestal are taken to be the ion neoclassical thermal conductivity, calculated at the top of the pedestal using the NCLASS model [18]. This simplification is motivated by the fact that the pedestal width is usually of the order of the ion orbit width (or banana width), which implies limited variation of the neoclassical transport across the barrier. A fixed pedestal width of 3 cm is assumed in the simulations carried out in this paper.

Edge boundary conditions are imposed at the separatrix for the ion density and for the electron and ion temperatures. The electron and ion temperature at the separatrix are taken to be 20 eV, and the ion density at the separatrix is assumed to be 1×10^{19} m^{-3}. It is found that the values used in the simulations for the electron and ion temperature at the separatrix do influence the time evolution of the ELMs, but do not affect the overall confinement.

2.2. MHD STABILITY CODES

To justify the simplified models used to trigger ELM crashes in the JETTO code, MHD stability analyses are carried out using the HELENA and MISHKA codes [15]. The HELENA code is used to refine the equilibrium and to compute the stability of infinite-n ideal ballooning modes. The HELENA code takes plasma profiles and equilibrium information, generated by JETTO, and produces an equilibrium with the higher resolution that is needed for the MISHKA code. MISHKA is then used to evaluate the stability criteria for finite-n ballooning and low-n kink/peeling modes. In this study, the MISHKA stability analysis is carried out for modes with toroidal mode number

$n = 1$ to $n = 14$. The version of the MISHKA code used in this paper is based on the ideal MHD model.

3. MODELS FOR TRIGGERING ELMS

In the JETTO simulations, the reduced transport within the pedestal region results in the development of a steep pressure gradient, which causes an increase in the bootstrap current within the pedestal. The increase of edge pressure gradient, and the resulting increase in the edge current density, leads to a destabilization of either a pressure-driven ballooning mode or a current-driven peeling mode. The resulting MHD instability triggers an ELM crash with an associated loss of plasma energy and particles to the wall.

The criterion used in the JETTO code for an ELM crash triggered by a pressure-driven ballooning mode is that the normalized pressure gradient, α, at any location within the pedestal region exceeds a critical value, α_c. That is

$$\alpha \equiv -\frac{2\mu_0 q^2}{\epsilon B_T^2}\frac{\partial p}{\partial \rho} > \alpha_c. \tag{1}$$

where μ_0 is the permeability of free space, q is the safety factor, ϵ is the inverse aspect ratio, B_T is the toroidal magnetic field, and $\partial p/\partial \rho$ is the pressure gradient. Note that α_c is a number determined as a result of stability analyses carried out using the HELENA and MISHKA codes.

The criterion for an ELM crash triggered by a current-driven peeling mode is that the current density anywhere within the pedestal exceeds a critical current density. This critical current density model is based on an analytical expression developed in Ref. [1]. For axisymmetric toroidal geometry, the current-driven peeling instability condition is

$$\sqrt{1 - 4D_M} + C < 1 + \frac{2}{2\pi q'}\oint \frac{j_\parallel B_T}{R^2 B_p^3} dl \tag{2}$$

where D_M is the Mercier coefficient, which is proportional to pressure gradient; C is a parameter related to the vacuum energy, which is taken to be 0.2 for the baseline simulations in this study; q' is the derivative of the safety factor with respect to the poloidal flux; $j_\parallel$ is the current density parallel to the magnetic field $\mathbf{B}$; R is the major radius; B_p is the poloidal magnetic field; and dl is the poloidal arc length element for the integral around a flux surface.

When the condition for an ELM crash is satisfied either by the pressure-driven ballooning mode criterion (Eq. 1) or by the current-driven peeling mode criterion (Eq. 2), an ELM crash in the JETTO simulation is produced as follows: The diagonal transport coefficients for electron and ion thermal transport within the pedestal are temporarily increased to 300 times the ion neoclassical diffusivity at the top of the pedestal, while the particle transport coefficients in the pedestal are increased to 100 times the ion neoclassical diffusivity at the top of the pedestal. The increased levels of transport are maintained for a time interval $\tau_{\mathrm{ELM}} = 0.4$ msec, which is of the order of a typical type-I ELM crash duration in JET. The large increase of the transport within the pedestal leads to a loss of particles and energy, comparable to the loss during an ELM crash in experiment.

4. RESULTS AND DISCUSSION

The simulation is carried out for the plasma parameters similar to those of JET discharge 44013 [19]; *i.e.*, major radius $R = 2.91$ m, minor radius $a = 0.94$ m, toroidal magnetic field $B_T = 2.76$ tesla, plasma current $I_p = 2.57$ MA, elongation $\kappa = 1.75$, and triangularity $\delta = 0.22$. During the quasi-stationary H-mode phase of the discharge, the line averaged electron density is 5.82×10^{19} m^{-3}, the neutral beam injected heating power is 13.9 MW, and $Z_{\rm eff}$ is 2.14.

4.1. JETTO SIMULATION

Figure 1 shows the time history of the ion diffusivity at the radius that corresponds to the top of the pedestal. The rapid increase of the ion diffusivity at this radius indicates an ELM crash in the JETTO simulation. It is found in the simulation that what appear to be individual ELM crashes in Fig. 1 are, in fact, sequences of quasi-continuous small ELM crashes separated by relatively longer ELM-free periods. In the sequence of ELM crashes at 17.73 s, for example, the first ELM crash is triggered by a pressure-driven ballooning mode while the remaining ELM crashes in that sequence are triggered by current-driven peeling modes. The details of this sequence of ELM crashes will be discussed below. A similar sequence of ELM crashes occurs at 17.97 s. On the other hand, ELM crashes in the remaining ELM sequences shown in Figure 1 are triggered only by current-driven peeling modes.

In Fig. 2, the ion diffusivity at the top of the pedestal during the first sequence of ELM crashes in Fig. 1 is plotted as a function of time using an expanded time scale. It can be seen that this sequence of ELM crashes consists of 5 individual ELM crashes, each 0.4 msec long (as is prescribed by the JETTO code). The first ELM crash in this sequence is triggered by a pressure-driven ballooning mode, that is as a consequence of the condition given in Eq. 1, while the rest of the ELM crashes are triggered by current-driven peeling modes, that is as a consequence of the condition given in Eq. 2.

The sequence of ELM crashes can be understood as follows: After the first ELM crash occurs, the edge pressure gradient decreases significantly, which results in a lower value of D_m (which is proportional to the pressure gradient) in Eq. 2. This decrease in the value of D_m results in a lower value for the critical current density needed to drive a peeling instability ($J_{||}$ on the right hand side of Eq. 2). The model for the ELM crash used in the study is diffusive, in that transport within the pedestal is rapidly increased to a high value during an ELM crash. This does not directly affect neo-classical plasma resistivity (apart from the temperature dependence), and, as a result, the current density in the pedestal is decreased only slightly during the first ELM crash of the sequence. Since the value of D_m, which is proportional to the pressure gradient, is significantly reduced during the first ELM crash, the current density that remains in the pedestal region is still large enough to trigger the peeling instability, which leads to subsequent ELM crashes. Gradually, the pedestal current density is reduced by resistive diffusion until the current-driven peeling mode

criterion given in Eq. 2 is no longer satisfied, and the sequence of ELM crashes comes to an end. The observation about the trigger for ELM crashes that the pressure-driven ballooning mode is unstable first and then the current-driven peeling mode becomes unstable is similar to the ELM model proposed in Ref. [20, 21].

Fig. 3 shows the time history of pressure and current density at normalized radius $\rho = 0.97$ during the ELM crash sequence shown in Fig. 2. Note that the normalized radius $\rho = 0.97$ is located in the middle of the pedestal region. It can be seen that the pressure within the pedestal decreases rapidly during the first ELM crash, while the current density in the middle of the pedestal at $\rho = 0.97$ decreases gradually during the sequence of ELM crashes. In Fig. 4, the radial profiles are plotted from $\rho = 0.50$ to the edge of the plasma for the plasma pressure and the current density at several times during the initial ELM crash sequence shown in Figs. 2 and 3. It can be seen that at $t = 17.7338$ s, which is the time just after the first ELM crash in that sequence, the pressure decreases significantly in the region between $\rho = 0.85$ and $\rho = 1.00$ ($\rho = 1.00$ is at the separatrix) compared with the pressure at $t = 17.7334$ s, which is the time just before the first ELM crash. In comparison, the edge current density at $t = 17.7338$ s decreases only slightly compared with the current density at $t = 17.7334$ s. After 5 consecutive ELM crashes, the edge current density decreases sufficiently so that the current-driven peeling modes are no longer unstable at 17.7359 s. This sequence of ELM crashes results in a total ELM crash duration of 2 msec.

4.2. SENSITIVITY OF ELM HISTORY TO VARIATIONS IN THE CONDITIONS FOR TRIGGERING ELMS AND TO THE VALUE OF THE SEPARATRIX TEMPERATURE

4.2.1. Variation of α_c

As mentioned in Sect. 3, the value of the critical pressure gradient, α_c, in the JETTO code is a prescribed number that is calibrated by stability analyses carried out using the HELENA and MISHKA stability codes. It is found in the JETTO simulations that the choice of the pressure gradient limit, α_c, influences the time evolution of ELMs.

A simulation is carried out in which α_c is 13% lower than the value of α_c used to obtain the results presented in Fig. 1. The time history of the ion diffusivity at the radius that corresponds to the top of the pedestal is shown in Fig. 5. It is found that the frequency of the ELM sequences increases as α_c decreases. The frequency of the ELM sequences in Fig. 1 is 4.75 Hz, while the frequency of the ELM sequences shown in Fig. 5 (the simulation result for which α_c is decreased) is 5.75 Hz. In all the sequences of ELM crashes shown in Fig. 5, the initial ELM of each sequence is triggered by a pressure-driven ballooning mode while the remaining ELMs in that sequence are triggered by current-driven peeling modes. This is in contrast to the results of the simulation presented in Fig. 1 where after the second ELM sequence all the subsequent ELMs are triggered only by current-driven peeling modes.

4.2.2. *Variation of parameter C*

The parameter C in Eq. 2, for an ELM crash triggered by a current-driven peeling mode, is related to the vacuum energy. It is found in the JETTO simulations that the choice of the parameter C influences the time evolution of ELMs. In this subsection, the effect of increasing the value of this parameter is examined.

Fig. 6 shows the time history of the ion diffusivity at the radius that corresponds to the top of the pedestal for the simulation using $C = 1.0$, compared with using $C = 0.2$ in the other simulation results presented in this paper. All other parameters, including α_c, are kept the same as in the baseline simulation used to obtain the result presented in Fig. 1. It is found that as the value of the parameter C increases, the ELM frequency increases. The ELM frequency increases from 4.75 Hz in Fig. 1 ($C = 0.2$) to 6.00 Hz in Fig. 6 ($C = 1.0$). It is also found that the number of ELM sequences that are triggered by a combination of pressure-driven ballooning and current-driven peeling modes is increased from 2 sequences in Fig. 1 ($C = 0.2$) to 8 sequences in Fig. 6 ($C = 1.0$).

The duration of longest ELM sequence becomes shorter as the parameter C is increased. In the simulation with $C = 0.2$, the duration of the longest ELM sequence is 3.6 msec and consists of 9 small ELM crashes. In contrast, in the simulation with $C = 1.0$, the duration of the longest ELM sequence is 1.6 msec and consists of 4 small ELM crashes. The shorter duration of the ELM sequence can be explained by the fact that a higher edge current density is required to destabilize a current-driven peeling mode as the parameter C is increased. As a result, less edge current needs to be removed to stabilize the current-driven peeling modes during each ELM crash sequence. Furthermore, since the ELM duration becomes shorter, the energy loss during each ELM sequence is reduced, resulting in less time needed to recover before the next ELM sequence. Consequently, the ELM frequency increases with the increase in the value of the parameter C.

4.2.3. *Variation of $T_{\rm sep}$*

It is found in the JETTO simulations that the temperature at the separatrix, $T_{\rm sep}$, has an influence on the time evolution of ELMs. The electron temperature, $T_{\rm e,sep}$, ion temperature, $T_{\rm i,sep}$, and ion density at the separatrix are imposed as boundary conditions in the JETTO simulations. The electron and ion temperature at the separatrix are set equal to each other in all of the simulations ($T_{\rm e,sep} = T_{\rm i,sep} = T_{\rm sep}$). In Fig. 7, the time history of the ion diffusivity at the top of the pedestal is plotted for simulations using $T_{\rm sep}$ of 20 eV (top panel), 100 eV (middle panel), and 200 eV (bottom panel). It can be seen that the duration of the ELM crash sequence in the simulation using $T_{\rm sep} = 20$ eV is briefer than the duration using $T_{\rm sep} = 200$ eV. Also, the frequency of the sequence of ELM crashes decreases from 4.75 Hz in the simulation using $T_{\rm sep} = 20$ eV to 3.50 Hz in the simulation using $T_{\rm sep} = 200$ eV.

As noted in Sect. 3, an ELM crash in the JETTO code is implemented by increasing the transport within the pedestal (300 times for thermal and 100 times for particle transport) during the crash.

The increased transport results in the rapid loss of temperature and particles, but not in the rapid loss of edge current density. In the JETTO code, the reduction of the current density occurs as a result of the resistive redistribution of the current density at the edge of the plasma. A higher edge resistivity, which is a consequence of a lower temperature, results in a more rapid reduction of the edge current density when an ELM crash occurs. The neo-classical expression for electrical resistivity, used in the JETTO code, is inversely proportional to the electron temperature. As a result, the edge current density changes more slowly during an ELM crash in a simulation with a high value of $T_{\rm sep}$ than that in a simulation with a low value of $T_{\rm sep}$. It is seen in Fig. 7 that the duration of each ELM crash decreases and the frequency of ELMs increases as the temperature at the separatrix is reduced. However, even with the low value of $T_{\rm sep}$ ($T_{\rm sep} = 20$ eV), the duration of ELM crashes is still higher than a typical experimentally observed ELM duration, which is usually less than 1 msec. Consequently, it would appear that an ELM crash triggered by a current-driven peeling mode can not be adequately described by a simple diffusive model for the redistribution of edge density and temperatures. To improve the agreement with the experimental results, either anomalous current diffusivity or dynamo effects are required. The discussion of those effects remain for future work. It is worth noting though that even with the present model, it is found that the temperature and density at the top of the pedestal before each composite ELM crash, as well as the thermal energy content and the global plasma confinement time, are nearly independent of $T_{\rm sep}$. The thermal energy content, $W_{\rm th}$, is shown as a function of time in Fig. 8 for simulations with $T_{\rm sep} =$ 20 eV, 100 eV, and 200 eV.

4.3. STABILITY ANALYSIS

In order to check the validity of the analytical ballooning stability criterion used in JETTO, the code is linked with the HELENA and MISHKA MHD stability analysis codes. The HELENA code uses, at a time just prior to an ELM crash, the self-consistent equilibrium produced by the JETTO code — that is the pressure gradient and the current density profiles together with the corresponding magnetic configuration. The HELENA code then reconstructs the equilibrium on a finer grid in order to provide the resolution required for the stability analysis. This refined equilibrium is used in the HELENA code to generate an infinite-n ballooning stability s-α diagram. Furthermore, a version of the MISHKA code, which is based on the ideal MHD model without dissipation or flow shear, is used to evaluate the stability criteria for finite-n ballooning and low-n kink/peeling modes. In this study, the stability analysis is carried out in the MISHKA code for toroidal mode numbers in the range of $n = 1$ to $n = 14$.

The results of the stability analyses carried out with the HELENA and MISHKA codes are presented in Fig. 9. In the top panel, the s-α stability diagram is shown at the time just prior to the first ELM crash in the first sequence of ELM crashes that appears in Fig. 1 ($t = 17.73$ s). In the bottom panel, the s-α stability diagram is shown at the time just prior to the first ELM crash in the sixth sequence of ELM crashes that appears in Fig. 1 ($t = 18.97$ s). In each panel, the stability

s-α diagram is plotted for the flux surface at normalized radius $\rho = 0.95$. The circle symbol represents the location of the operational point, given by the JETTO code, for the pressure gradient and magnetic shear at that flux surface. The region of instability associated with the infinite-n ideal ballooning modes is indicated with crosses, while the numbers on these plots indicate the toroidal mode number of the most unstable finite-n ballooning and low-n kink/peeling modes at each location on the s-α plane.

It can be seen that the pedestal pressure gradient at $t = 17.73$ s is close to the region of the infinite-n ballooning mode (indicated by crosses), but also not far from the region of low-n kink mode. Note that it is found in the JETTO simulation that the first ELM crash of the sequence of ELM at $t = 17.73$ s is triggered by a pressure-driven ballooning mode. It can also be seen that the ELM at $t = 18.97$ s (just before the sixth sequence of ELM crashes in Fig. 1) is triggered by a low-n kink mode ($n = 4$). This result is also consistent with the JETTO simulation described in Section 4.1 in that the first ELM crash of the sequence of ELM at $t = 18.97$ s is triggered by a current-driven peeling mode.

5. CONCLUSION

The time evolution of ELMs is investigated. It is found in the JETTO simulations that stability criteria based on pressure-driven ballooning modes and current-driven peeling modes both play a role in triggering ELM crashes. In the simulations, each ELM crash consists of a sequence of ELM crashes. The initial crash in each ELM sequence can be triggered either by a pressure-driven ballooning mode or by a current-driven peeling mode. After the initial crash, subsequent crashes within each sequence are triggered by current-driven peeling modes, which are made more unstable by the reduction in the pressure gradient caused by the initial crash. The choice of the critical pressure gradient for a pressure-driven ballooning mode, the parameter related to the vacuum energy, and temperature at the separatrix all have an influence on the time evolution of ELMs, but they do not affect the global plasma confinement in the simulation results.

ACKNOWLEDGMENTS

T. Onjun thanks the Royal Thai Government and the Development and Promotion for Science and Technology Talents Project of Thailand (DPST) for their support. T. Onjun also thanks Dr. Alexie Pankin for his comments on this paper. This work was conducted partly under European Fusion Development Agreement. It was supported in part by the U.S. Department of Energy (DOE) under contract No. DE-FG02-92-ER-5414 and by the UK Department of Trade and Industry and by EURATOM.

REFERENCES

[1] J. W. Connor, H. R. Hastie, H. R. Wilson, and R. L. Miller, Phys. Plasmas **5**, 2687 (1998).

[2] J. Kinsey, T. Onjun, G. Bateman, A. H. Kritz, A. Pankin, G. M. Staebler, and R. E. Waltz, Nucl. Fusion **43**, 1845 (2003).

[3] R. Aymar, P. Barabaschi, and Y. Shimomura, Plasma Phys. Control. Fusion **44**, 519 (2002).

[4] H. R. Wilson, J. W. Connor, A. R. Field, S. J. Fielding, R. L. Miller, L. L. Lao, J. R. Ferron, and A. D. Turnbull, Phys. Plasmas **6**, 1925 (1999).

[5] P. Gohil, Phys. Rev. Letters **61**, 1603 (1988).

[6] G. T. A. Huysmans, T. C. Hender, and B. Alper, Nucl. Fusion **38**, 179 (1998).

[7] G. T. A. Huysmans, T. C. Hender, B. Alper, *et al.*, Nucl. Fusion **39**, 1489 (1999).

[8] H. R. Wilson and R. L. Miller, Phys. Plasmas **6**, 873 (1999).

[9] J. Manickam, Phys. Fluids **B4**, 1901 (1992).

[10] J. S. Lonnroth, V. V. Parail, G. Corrigan, *et al.*, Plasma Phys. Control. Fusion **45**, 1689 (2003).

[11] V. V. Parail, G. Bateman, M. Becoulet, *et al.*, Plasma Physics Reports **29**, 539 (2003).

[12] T. Onjun, A. H. Kritz, G. Bateman, V. Parail, J. Lonnroth, and G. Huysmans, *Integrated Pedestal and Core Modeling of JET Triangularity Scan Discharges*, submitted to Phys. Plasmas .

[13] G. W. Pacher, H. D. Pacher, A. S. Kukushkin, G. Janeschitz, and G. Pereverzev, Nucl. Fusion **43**, 188 (2003).

[14] T. Onjun, A. H. Kritz, G. Bateman, V. Parail, H. Wilson, J. Lonnroth, G. Huysmans, and A. Dnestrovskij, *Stability Analysis of H-mode Pedestal and ELMs in a JET Power Scan*, to appear in Phys. Plasmas .

[15] A. B. Mikhailovskii, G. T. A. Huysmans, S. E. Sharapov, and W. Kerner, Plasma Phys. Rep **23**, 844 (1997).

[16] G. Cenacchi and A. Taroni, JET-IR(88) **03** (1988).

[17] M. Erba, A. Cherubini, V. V. Parail, and A. Taroni, Plasma Physics and Controlled Fusion **39**, 261 (1997).

[18] W. A. Houlberg, K. C. Shaing, S. P. Hirshman, and M. C. Zarnstorff, Phys. Plasmas **4**, 3231 (1997).

[19] G. Saibene, L. D. Horton, R. Sartori, *et al.*, Nucl. Fusion **39**, 1133 (1999).

[20] H. R. Wilson, J. W. Connor, A. R. Field, R. J. Hastie, R. L. Miller, and J. B. Taylor, Nucl. Fusion **40**, 713 (2000).

[21] P. B. Snyder, H. R. Wilson, J. R. F. L. L. Lao, A. W. Leonard, T. H. Osbrone, A. D. Turnbull, D. Mossessian, M. Murakami, and X. Q. Xu, Phys. Plasmas **9**, 2037 (2002).

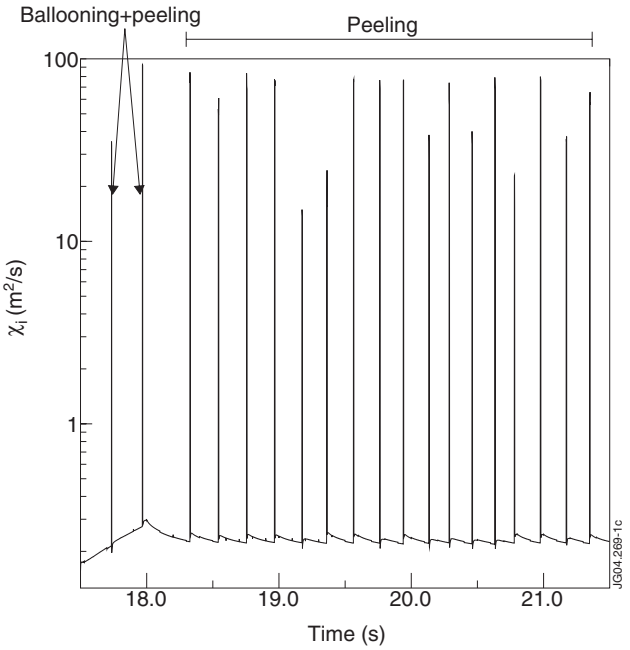

Figure 1: The time history of the ion diffusivity at location corresponding to the top of the pedestal is plotted between 17.5s and 21.5s. The rapid increase in the ion diffusivity at the top of the pedestal indicates an ELM crash sequence in the JETTO simulation. The first two sequences of ELM crashes include ELMs that are triggered by a combination of ballooning and peeling modes, while the remaining 17 ELM crash sequences that occur between 18.0s and 22.5s contain ELMS triggered only by the peeling mode.

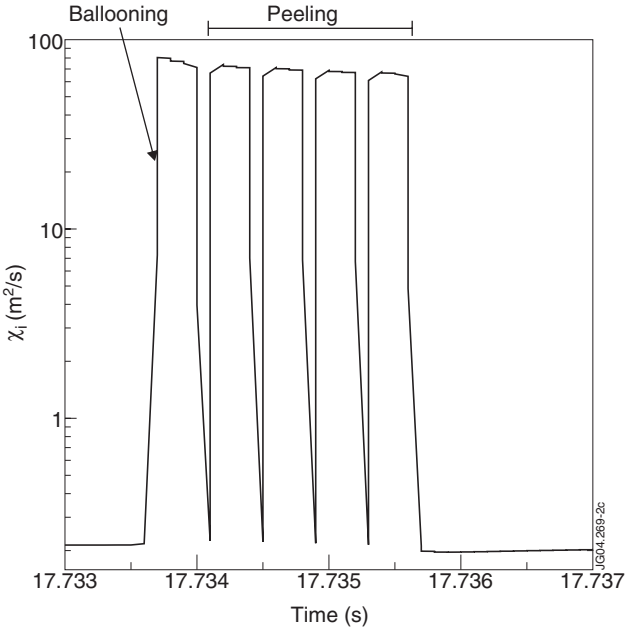

Figure 2: The ion diffusivity at the top of the pedestal is plotted as a function of time for the first sequence of ELM crashes shown in Fig. 1. In this sequence of 5 ELM crashes, the first ELM crash is triggered by a pressure-driven ballooning mode while the subsequent ELM crashes in this sequence are triggered by a current-driven peeling mode.

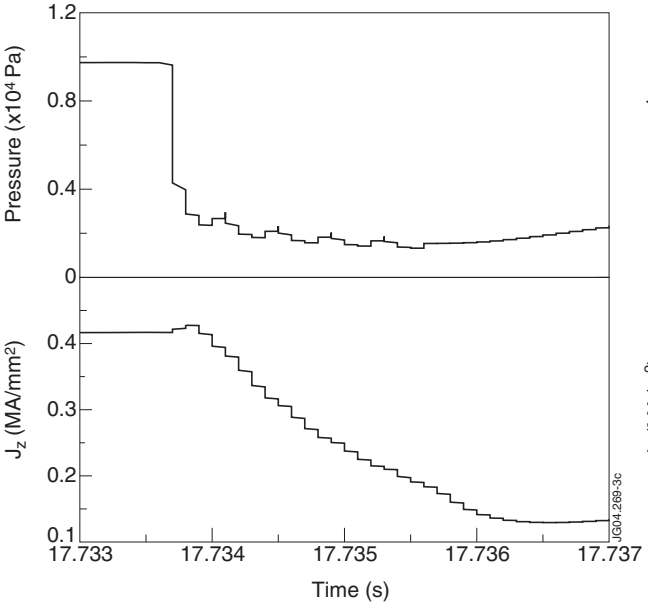

Figure 3: The simulated plasma pressure and plasma current density, J_z, at the normalized radius $\rho = 0.97$, are plotted as a function of the time during the sequence of ELM crashes shown in Fig.2.

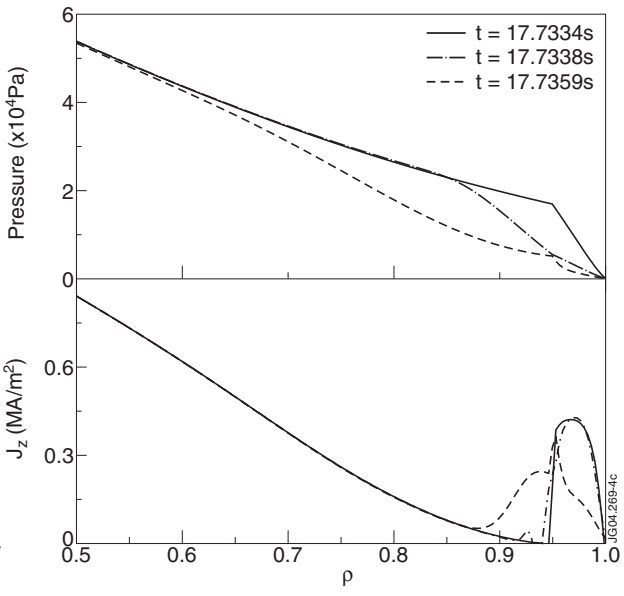

Figure 4: Plasma pressure and current density profiles are plotted at three times during the first sequence of ELM crashes shown in Fig.2. The solid line shows the profiles at t = 17.7334s, just before the first ELM crash of the sequence. The chained line shows the profiles at t = 17.7338s, just after the first ELM crash. The dashed line shows the profiles at t = 17.7359s, after the end of the sequence of the 5 ELM crashes.

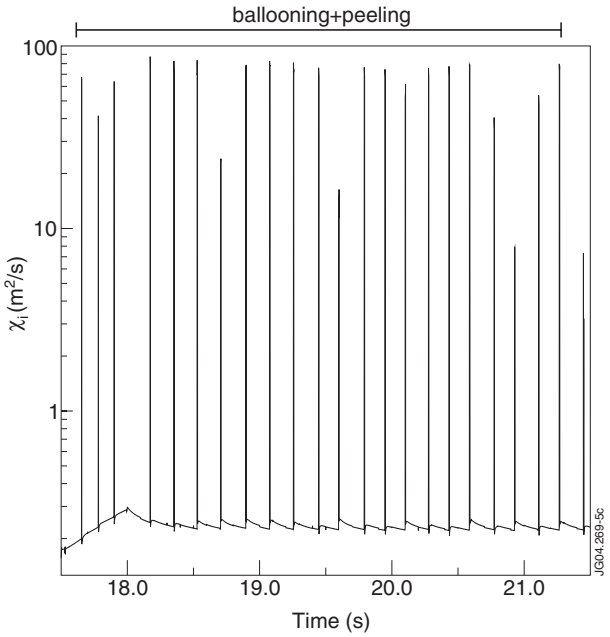

Figure 5: The time history of the ion diffusivity at the top of the pedestal is plotted between 17.5s and 21.5s. This simulation is carried with the pressure gradient limit that is 13 % lower than the pressure gradient limit used in Fig.1. All of the 23sequences of ELM crashes in this simulation are triggered by a combination of ballooning and peeling modes.

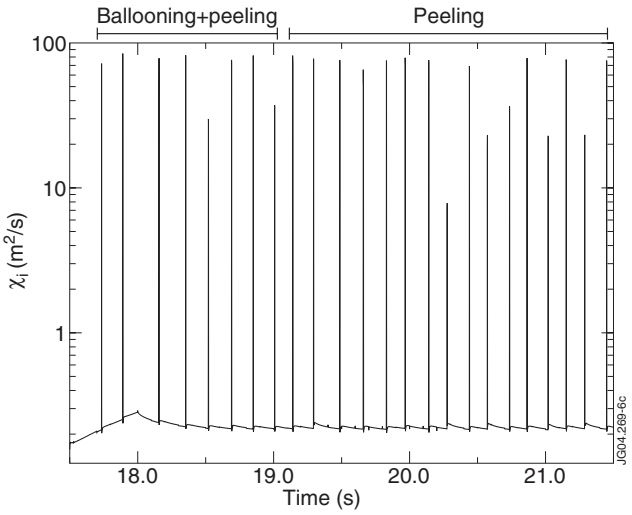

Figure 6: The time history of the ion diffusivity at the top of the pedestal is plotted between 17.5s and 21.5s. This simulation is carried with C = 1.0. The first 8 sequences of ELM crashes are triggered by a combination of ballooning and peeling modes, while the rest of the sixteen sequences of ELM crashes are triggered by peeling modes only.

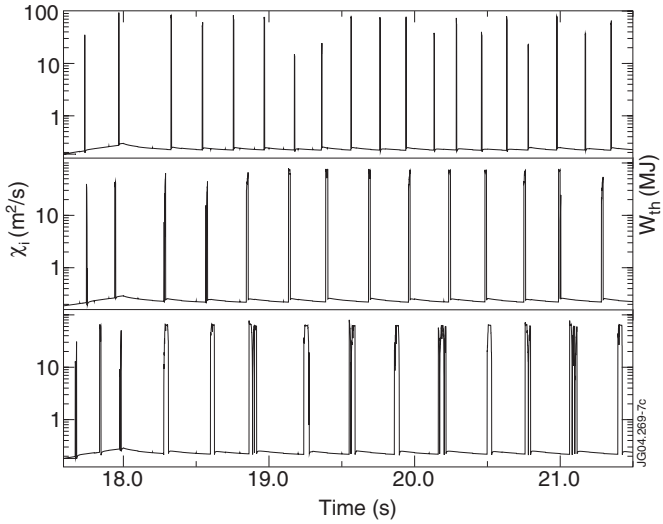

Figure 7: Ion diffusivity at the top of the pedestal as a function of time from a simulation using T_{sep} = 20 eV in the top panel, T_{sep} = 100 eV in the middle panel, and T_{sep} = 200eV in the bottom panel.

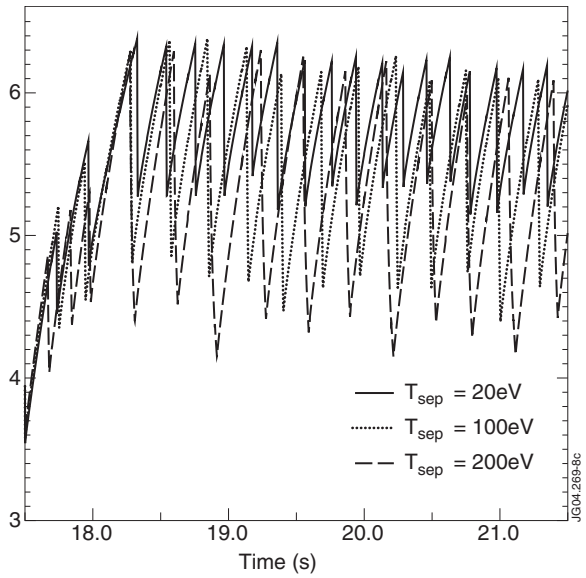

Figure 8: Thermal energy content, W_{th}, is plotted as a function of time from the simulations using T_{sep} = 20eV, T_{sep} = 100eV, and T_{sep} = 200eV. The peak values of thermal energy content before each sequence of ELM crashes are nearly the same in all the simulations. However, the minimum values of thermal energy content after each sequence of ELM crashes are different in the different simulations. This is a consequence of the longer duration of the ELM crash sequences in the simulations with higher T_{sep} .

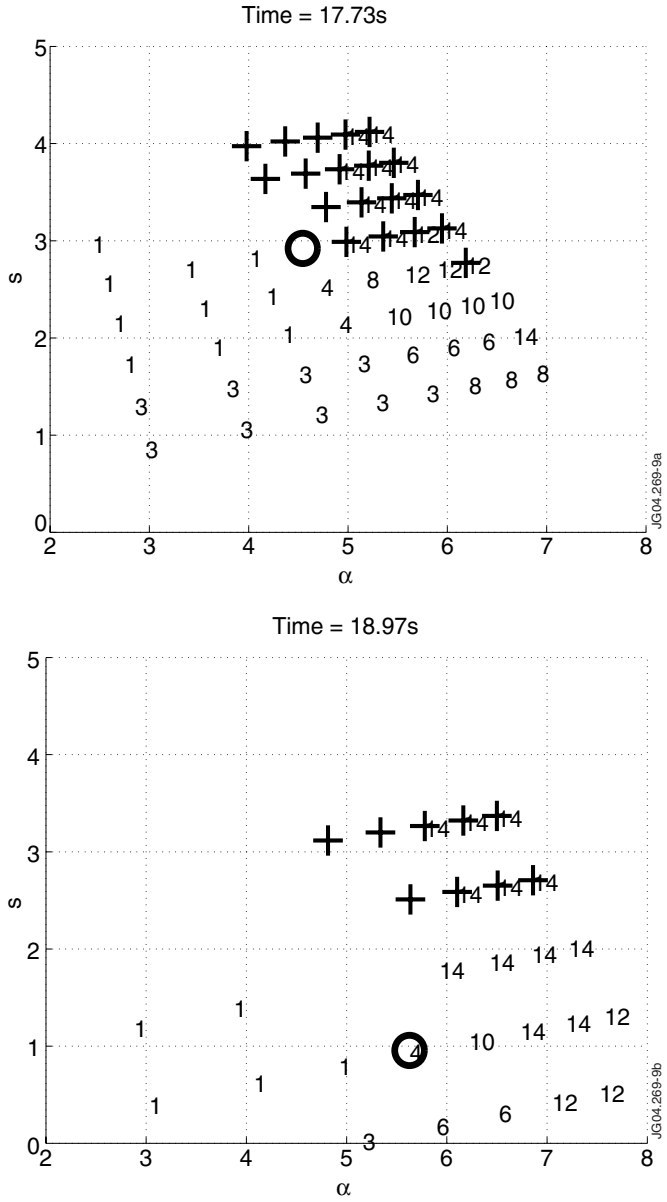

Figure 9: Stability results obtained using the HELENA and MISHKA codes are plotted for the flux surface at normalised radius $\rho = 0.95$ on an $s-\alpha$ stability diagram just befor the first ELM crash of the sequence that occurs at t = 17.73s (top panel) and at t = 18.97s (bottom panel). Crosses mark the region that is unstable to finite-n ideal ballooning modes. The numbers indicate the most unstable finite$-n$ ballooning and low-n kink/peeling modes at each location on the $s-\alpha$ plane. All of the modes are stable in the region without numbers or crosses.